High-Speed, Three-Dimensional Quantification of Ladybug (*Hippodamia convergens*) Flapping Wing Kinematics During Takeoff

Ryan B. George, Scott L. Thomson
Department of Mechanical Engineering, Brigham Young University, Provo, UT, 84602

Ladybug wing and body kinematics during takeoff is explored using high-speed stereoscopic images acquired at a rate of 3000 frames per second. A direct linear transformation algorithm is used to quantify positions of selected locations on the body, forewings (elytra), and hindwings. Design and setup of instrumentation and analysis procedures are explained. Flapping frequency is reported. Significant motion of the forewing and other findings are presented and their applications are discussed.

Nomenclature

[x y z]	=	Coordinates in Cartesian space (cm)
u_L, v_L	=	x, y position of object in left view frame (pixels)
u_R, v_R	=	x, y position of object in right view frame (pixels)
L	=	Left image calibration vector
R	=	Right image calibration vector
H	=	Homogeneous transformation

I. Introduction

The use of flapping flight is ubiquitous among the animal and insect kingdom[1]. Flapping flight, which features an aerodynamic flight regime characterized by a relatively low Reynolds number, yields lift-generating mechanisms. It introduces several advantages such as increased agility and ability to navigate in confined spaces (such as indoors). It also offers the potential for decreased detectability, due to reduced size and possible reduced noise, and the ability to hover.

Many aspects of flapping flight kinematics, both in natural and man-made systems, however, are yet to be fully understood. Such aspects include phenomena due to deformable and/or adjustable wings and wing kinematics, and the wide variability in wing size, wing shape, and wing and body kinematics. One particular aspect of interest is the influence of the forewings found in beetles (*Coleoptera*). Flying beetles such as ladybugs (*Hippodamia convergens*) have two stiff, protective forewings and two flapping hindwings. The forewings, known as elytra (or elytron, singular), cover the hindwings when not in flight, but move upward and forward during flight. They also perform other functions such as trapping moisture, protection, etc.[2] The role of the forewing during flight, however, has not been thoroughly explored; nor have the wing kinematics and aerodynamics of the forewing-hindwing combination.

The goal of the present research is to analyze beetle flapping wing kinematics using ladybugs as subjects. A series of high-speed images of a ladybug during takeoff to quantify the three-dimensional position of points on the body, forewings, and hindwings has been analyzed to quantify forewing opening, hindwing motion during flapping, and body motion during takeoff.

II. Methods

A. Overview

The approach of the present research is to analyze flapping wing kinematics using high-speed stereoscopic imaging. A direct linear transformation (DLT) is applied in order to correlate the two-dimensional stereoscopic image coordinates into three-dimensional Cartesian spatial coordinates. The goal is to convert this data into appropriate kinematic representations for use in investigating the role of the forewing in flapping flight and to study deformable wing shape kinematics of ladybugs.

B. Data Acquisition

As illustrated in Fig. 1, the experimental setup involves a Photron APX-RS high-speed digital camera, a mirror arrangement for projecting two views of an object onto a single camera image, and a combination of LED and incandescent lighting. The frame rate of the camera is set to 3000 frames per second while the shutter speed is $1/6000^{th}$ of a second. This higher shutter speed ensures a relatively complete freeze of the wing motion. A Nikon 105mm Nikkor lens is used with an aperture of F11.

Prior to image acquisition, a calibration target was created using $1/16^{th}$ inch diameter extruded wire soldered together to form a grid pattern. The target consists of 5 tiers with 25 white dots painted on each tier, providing a total of 125 calibration points. The target was placed in the camera's field of view, so that two views of the target are visible in the camera image (see Fig. 2).

C. Data Analysis

Matlab is the primary tool used to analyze the high-speed images. A Direct Linear Transformation (DLT) implementation, custom coded in Matlab, is used. The DLT is here briefly described; further details can be found elsewhere[3,4].

DLT is a method of determining the three dimensional location of an object (or points on an object) in space using two different views of the object. There are a variety of ways of attaining multiple images; however, the approach used here is one camera and an arrangement of mirrors. This allows for the relative distances between the camera, mirrors, and object to be varied over a sufficiently wide range. This method is also beneficial since it requires only a single camera and requires no temporal synchronization between sets of images.

Calibration is found using 100 visible calibration points on the aforementioned calibration target. Calibration consists of finding vectors **L** and **R** using the following series of equations. First,

$$\begin{bmatrix} x_1 & y_1 & z_1 & 1 & 0 & 0 & 0 & 0 & -u_{L1}x_1 & -u_{L1}y_1 & -u_{L1}z_1 \\ 0 & 0 & 0 & 0 & x_1 & y_1 & z_1 & 1 & -v_{L1}x_1 & -v_{L1}y_1 & -v_{L1}z_1 \\ x_2 & y_2 & z_2 & 1 & 0 & 0 & 0 & 0 & -u_{L2}x_2 & -u_{L2}y_2 & -u_{L2}z_2 \\ 0 & 0 & 0 & 0 & x_2 & y_2 & z_2 & 1 & -v_{L2}x_2 & -v_{L2}y_2 & -v_{L2}z_2 \\ & & & & & \vdots & & & & & \\ x_N & y_N & z_N & 1 & 0 & 0 & 0 & 0 & -u_{LN}x_N & -u_{LN}y_N & -u_{LN}z_N \\ 0 & 0 & 0 & 0 & x_N & x_N & x_N & 1 & -v_{LN}x_N & -v_{LN}y_N & -v_{LN}z_N \end{bmatrix} \begin{bmatrix} L_1 \\ L_2 \\ L_3 \\ L_4 \\ L_5 \\ L_6 \\ L_7 \\ L_8 \\ L_9 \\ L_{10} \\ L_{11} \end{bmatrix} = \begin{bmatrix} u_{L1} \\ v_{L1} \\ u_{L2} \\ v_{L2} \\ \vdots \\ u_{LN} \\ v_{LN} \end{bmatrix}, \quad (1)$$

is calculated, where N is the number of calibration points, x_i, y_i, and z_i (i = 1 to N) are the known positions of the calibration points, u_{Li} and v_{Li} are the horizontal and vertical pixel locations, respectively, of the points in the images, and L_1 through L_{11} are the calibration constants. Similarly, **R** (R_1 through R_{11}) is found by replacing v_{Li}, v_{Li}, and L with u_{Ri}, v_{Ri}, and **R**. If we denote the first matrix on the left-hand side as $\mathbf{F_L}$ and the right-hand side matrix as $\mathbf{g_L}$, then using the Moore-Penrose pseudo-inverse method, we can write

$$\mathbf{L} = \left(\mathbf{F_L^T F_L}\right)^{-1} \mathbf{F_L^T g_L}, \quad (2)$$

and similarly for **R**

$$\mathbf{R} = \left(\mathbf{F_R^T F_R}\right)^{-1} \mathbf{F_R^T g_R}. \quad (3)$$

The position of any point visible from two perspectives in the image can then be found using the equation

$$\begin{bmatrix} L_1 - L_9 u_L & L_2 - L_{10} u_L & L_3 - L_{11} u_L \\ L_5 - L_9 v_L & L_6 - L_{10} v_L & L_7 - L_{11} v_L \\ R_1 - R_9 u_R & R_2 - R_{10} u_R & R_3 - R_{11} u_R \\ R_5 - R_9 v_R & R_6 - R_{10} v_R & R_7 - R_{11} v_R \end{bmatrix} \begin{bmatrix} x \\ y \\ z \end{bmatrix} = \begin{bmatrix} u_L - L_4 \\ v_L - L_8 \\ u_R - R_4 \\ v_R - R_8 \end{bmatrix}. \quad (4)$$

Denoting the first matrix on the left-hand side as **Q** and the right-hand side matrix as **q**, Eq. (4) can be written as

$$\mathbf{Q} \begin{bmatrix} x \\ y \\ z \end{bmatrix} = \mathbf{q}, \quad (5)$$

from which the Moore-Penrose pseudo-inverse method can be applied to find the position of the unknown Cartesian coordinates x, y, and z:

$$\begin{bmatrix} x \\ y \\ z \end{bmatrix} = \left(\mathbf{Q^T Q}\right)^{-1} \mathbf{Q^T q}. \quad (6)$$

In the present research, the **L** and **R** calibration matrices are found using the calibration target. A ladybug is then placed in the field of view and images of the ladybug are acquired during takeoff. The x, y, and z locations of four points on the ladybug are then tracked. The points include a point near the front of the body, a point near the rear of the body, and the tip of both forewings and hindwings.

Once 3D Cartesian spatial coordinates have been found, a set of homogeneous matrices can be applied in order to analyze data in a more relative plane. This is accomplished via use of a rotation transformation, contained in a 3x3 sub-matrix of the homogeneous transformation (**H**), which we will denote by **T**. A rotation by θ_z in the z-axis, a rotation by θ_y in the y-axis and a rotation by θ_x in the x-axis, respectively, can be represented by

$$\mathbf{T}(\theta_z, \theta_y, \theta_x) = \begin{bmatrix} 1 & 0 & 0 \\ 0 & \cos\theta_x & -\sin\theta_x \\ 0 & \sin\theta_x & \cos\theta_x \end{bmatrix} \quad (7)$$

$$\begin{bmatrix} \cos\theta_y & 0 & \sin\theta_y \\ 0 & 1 & 0 \\ -\sin\theta_y & 0 & \cos\theta_y \end{bmatrix} \begin{bmatrix} \cos\theta_z & -\sin\theta_z & 0 \\ \sin\theta_z & \cos\theta_z & 0 \\ 0 & 0 & 1 \end{bmatrix}$$

The translation transformation is represented by

$$\mathbf{p} = \begin{bmatrix} x \\ y \\ z \end{bmatrix}, \quad (8)$$

where x ,y ,z is the vector representing the location from the origin of the initial frame to the origin of the new relative frame. Homogeneous matrix H when matrix multiplied with the 3D Cartesian coordinate, results in the new resolved Cartesian coordinate

$$[x_{new}, y_{new}, z_{new}, 1] = \begin{bmatrix} \mathbf{T} & & & \mathbf{p} \\ (3x3) & & & (3x1) \\ & & & \\ 0 & 0 & 0 & 1 \end{bmatrix} \begin{bmatrix} x_{old} \\ y_{old} \\ z_{old} \\ 1 \end{bmatrix}. \quad (9)$$

Each data set was rotated manually using its own homogeneous matrix to allow analysis of flapping wing and body kinematics.

III. Results

Calibration of **L** and **R** vectors using the calibration target resulted in an average coordinate error of 0.147 cm. Figure 3 shows the known positions of the points on the calibration target. Returning the pixel locations of the calibration points into Eq. (6) allows for an estimate of the quality of the calibration data. The comparison between actual and calculated points is adequate.

DLT analysis has been performed on 5 data sets (all different ladybugs), or 1,344 frames of data. In each data set, both forewings, both hindwings, the front body, and rear body have been quantified. Figure 4 shows two images of the ladybug; one shortly after takeoff initiation, and another a short time later. These images show the coordinate system used.

Figure 5 plots a time history of the positions of the six points on the ladybug during takeoff. This demonstrates successful implementation of image analysis of the ladybug specimen. It is interesting to note that the forewing moves in unison with the hindwing with a relatively large amplitude. This may be a passive reflex, although further investigation is required to determine this.

Figure 6 shows an exploration of vertical displacement of both forewing and hindwing. It is apparent that a brief *y*-direction reversal occurs in the middle of the flapping stroke cycle when the hindwing transitions shape. Figure 7 shows a comparison of this phenomenon overlayed with video images to visualize what is taking place.

Figure 8 shows the hindwing elevation (*z*-position) vs. time. A flapping frequency analysis shows an average flapping frequency of 78.6 Hz (see Table 1). Figure 9 shows results from an analytical analysis of body velocity. Results indicate that the specimen is traveling at an average velocity of about 21.4 cm/second.

Table 1. Frequency of ladybug flapping.

Period	Time (Seconds)	Frequency (Hz)
T_1	0.01267	78.9
T_2	0.01233	81.1
T_3	0.01367	73.2
T_4	0.01233	81.1
Average Frequency		78.6

Figure 10 displays a sequence of images which help visualize the flexible nature of the hindwing. Wing rotation and deformation is evident, as has been observed elsewhere; this allows the airfoil shape of the wing to produce lift over the bulk of the insect's flapping period and contributes to other lift-enhancing phenomena.

Figure 11 shows a ladybug during takeoff and transitioning into horizontal flight. It is observed that the amplitude of the stroke elevation is large, at first, and then transitions into smaller, steady, strokes. Figure 12 shows an exploration of vertical displacement of both forewing and hindwing.

Figure 13 shows a quantification of both forewings of a ladybug specimen during opening. This kinematic identification shows that these forewings do not simply follow a straight line approach to their takeoff position, but follow a curved path.

Finally, in Fig. 14, a unique behavior of the legs can be seen The 2nd image in the sequence show the legs moving outward and the 3rd image in the sequence show the legs in an almost fully extended position. We have consistently observed this phenomenon in ladybugs. The purpose for this behavior is currently unknown.

IV. Conclusion

The work presented represents results from data acquired from a series of high-speed images of a ladybug during takeoff. These results illustrate the functionality of the DLT implementation and calibration technique, the successful data acquisition of a ladybug in takeoff and free flight, and show analysis of several sequences of video image data. Data of this type may be useful in investigating the aerodynamics of insect flight, including the development and analysis of computational and experimental models. Of particular interest will be the aerodynamic interaction of the relatively stiff (but clearly not static) forewing-generated vortices with those generated by the much larger hindwings.

Acknowledgments

Support for R.G. of a research award from the Rocky Mountain NASA Space Grant Consortium is gratefully acknowledged.

References

[1]Shyy, W., Lian, Y., Tang, J., Viieru, D., and Liu, H. *Aerodynamics of Low Reynolds Number Flyers*, Cambridge University Press, Cambridge, 2008, Chapters 1,4.

[2]Frantsevich L, Zhendong D, Wang W, and Zhang Y. "Geometry of Elytra Opening and Closing in Some Beetles", *The Journal of Experimental Biology*, Vol. 208, 2005, pp. 3145-3158.

[3]Abdel-Azez, Y. I. and Karara, H. M. "Direct Linear Transformation from Comparator Coordinates into Object Space Coordinates in Close-Range Photgrammetry," *Proceedings of the ASP/UI Symposium on Close-Range Photogrammetry* (American Society of Photogrammetry, Falls Church, VA), 1971, pp. 1-18.

[4]Hartley, Richard. Zisserman, Andrew. *Multiple View Geometry in computer vision*, Cambridge University Press, Cambridge, 2003.

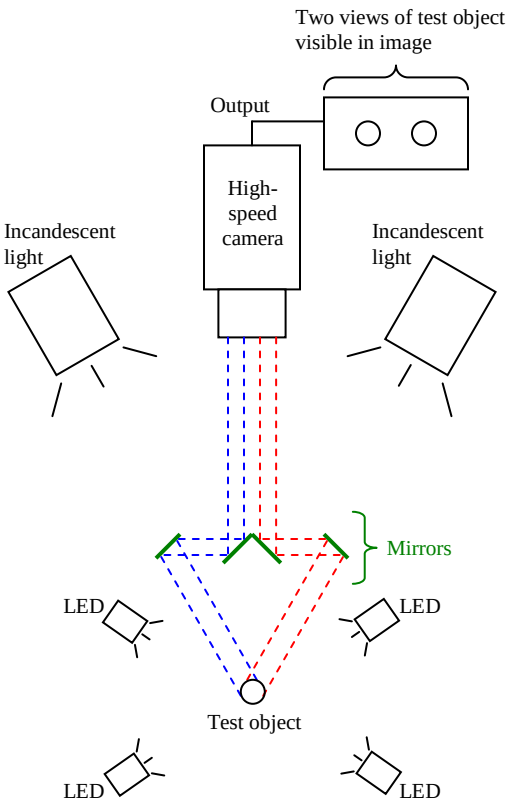

Figure 1. High-speed imaging setup.

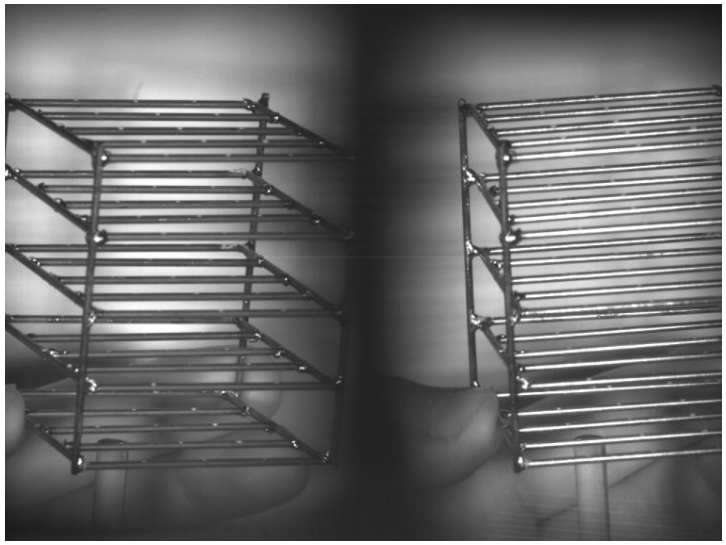

Figure 2. Calibration target as viewed using setup shown in Fig. 1.

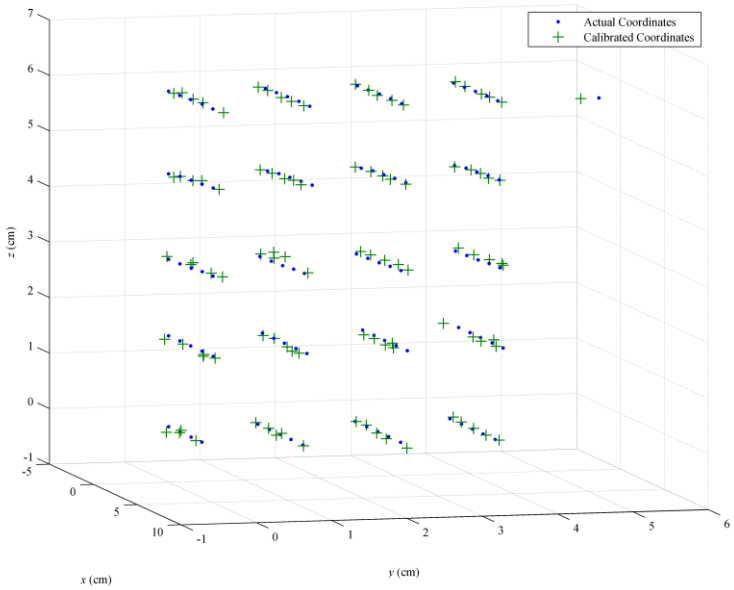

Figure 3. Calibration Target Results

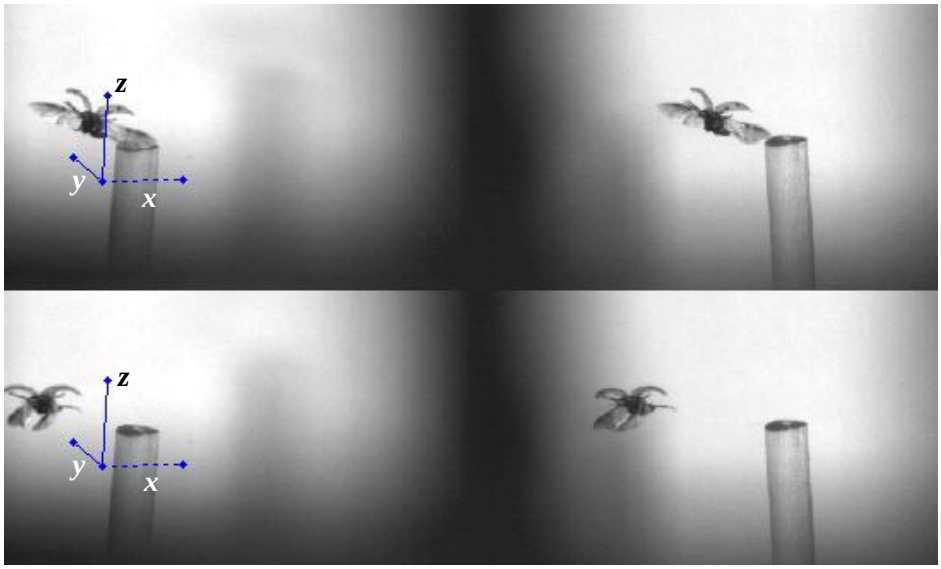

Figure 4. Image sequence showing first and last frame coordinate system.

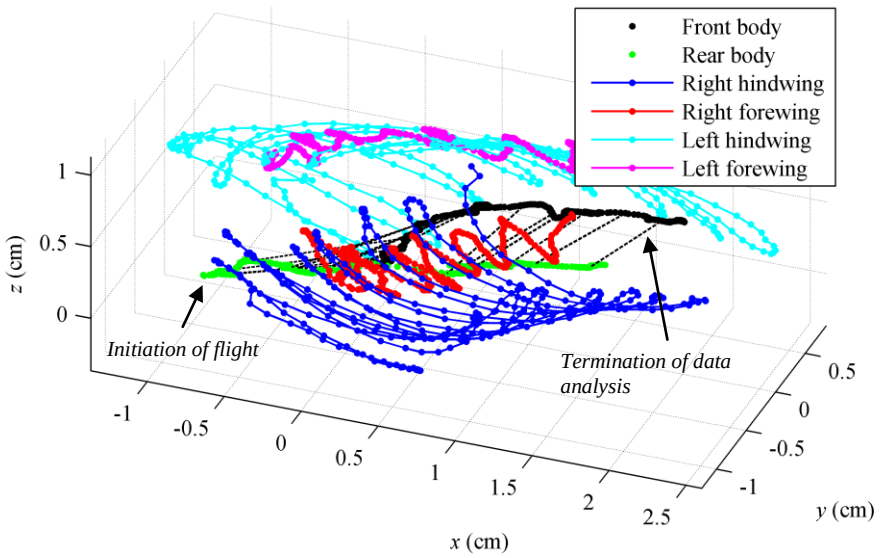

Figure 5. Symbols showing three-dimensional paths of six ladybug anatomical landmarks. The dashed black lines connect the front and rear body points, illustrating the approximate ladybug attitude, at select times.

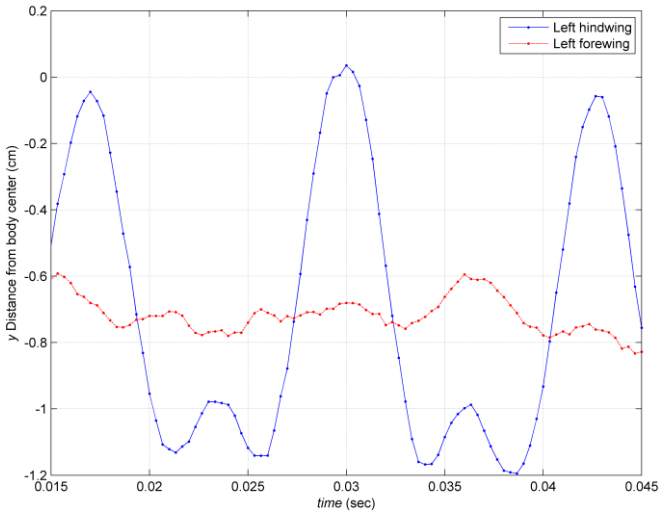

Figure 6. Horizontal (*y*) position of forewing and hindwing.

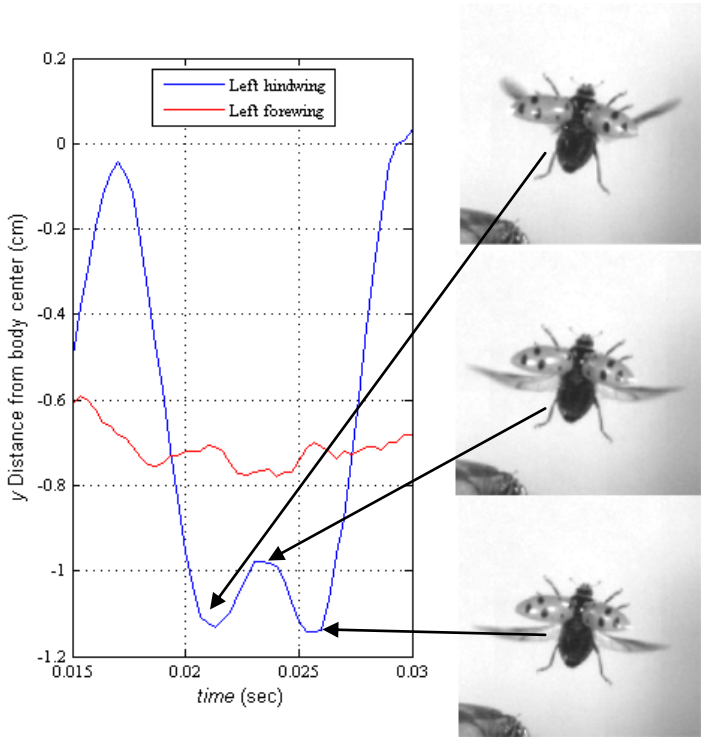

Figure 7. Visual exploration of flapping wing vs. video images.

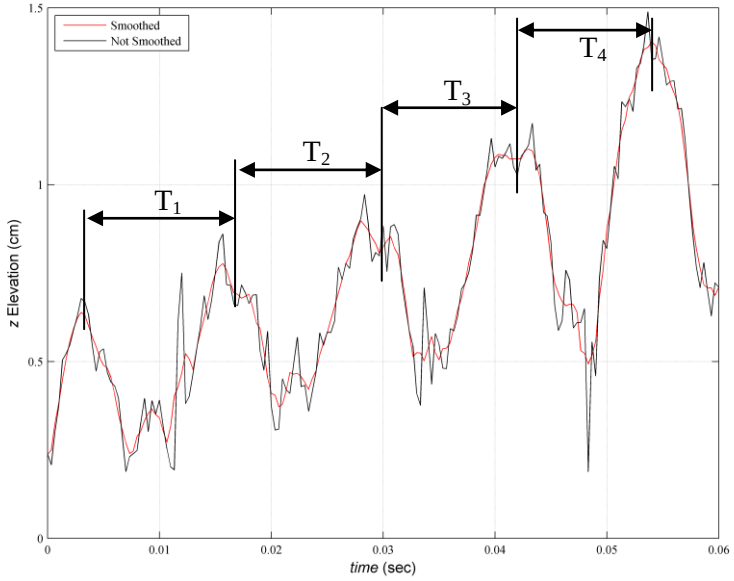

Figure 8. Hindwing elevation (*z*) vs. time.

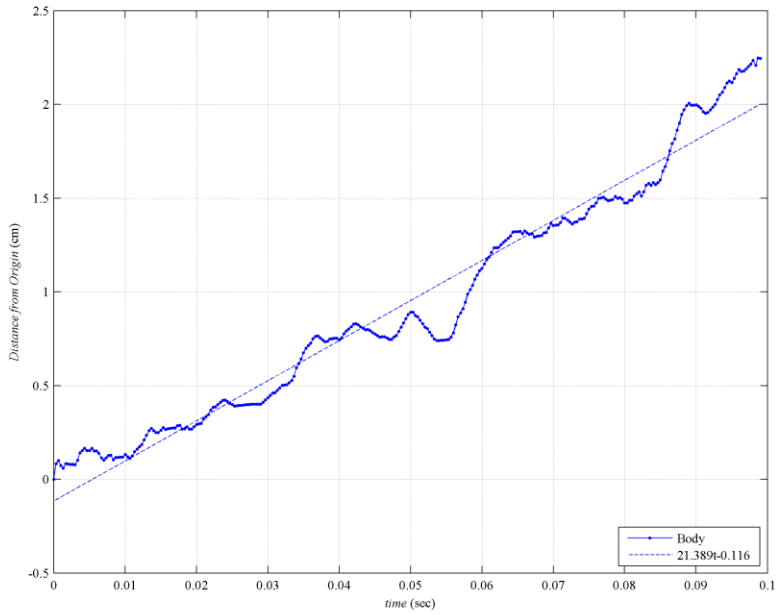

Figure 9. Body vertical displacement vs. time, along with linear curves fit to estimate average velocity.

Figure 10. Image sequence showing hindwing deformation.

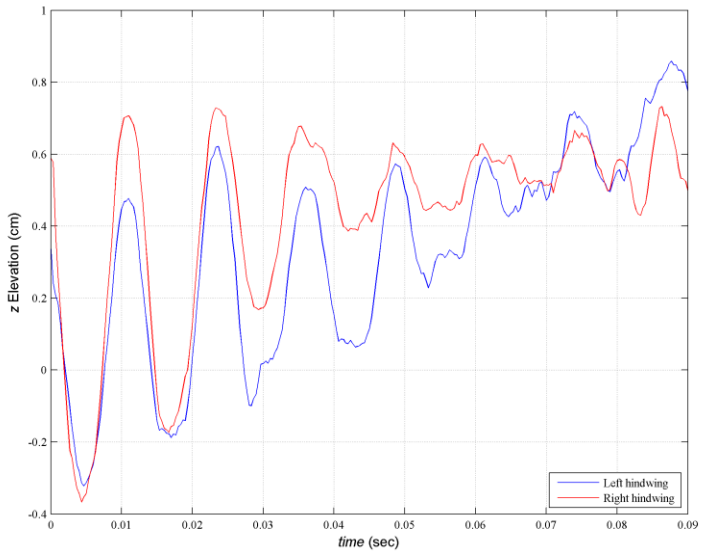

Figure 11. Ladybug wing amplitude steadily decreases as it transitions to steady flight.

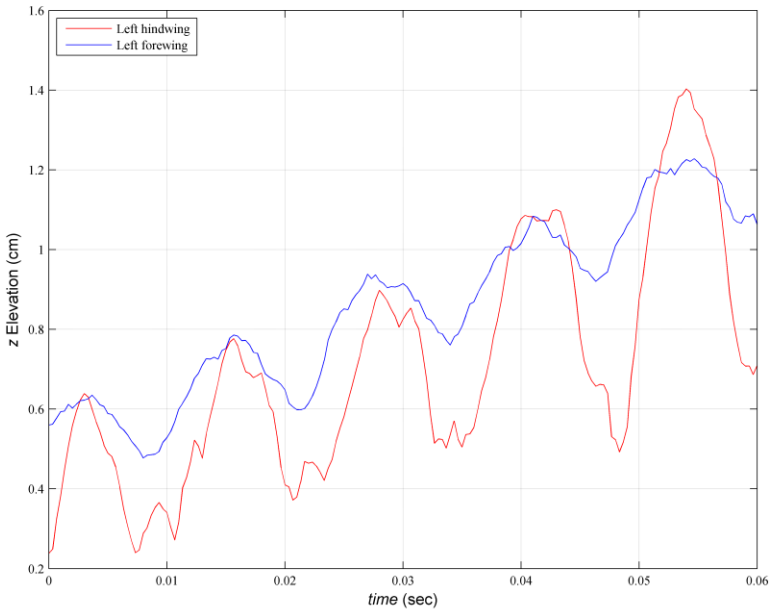

Figure 12. Vertical (*z*) position of forewing and hindwing.

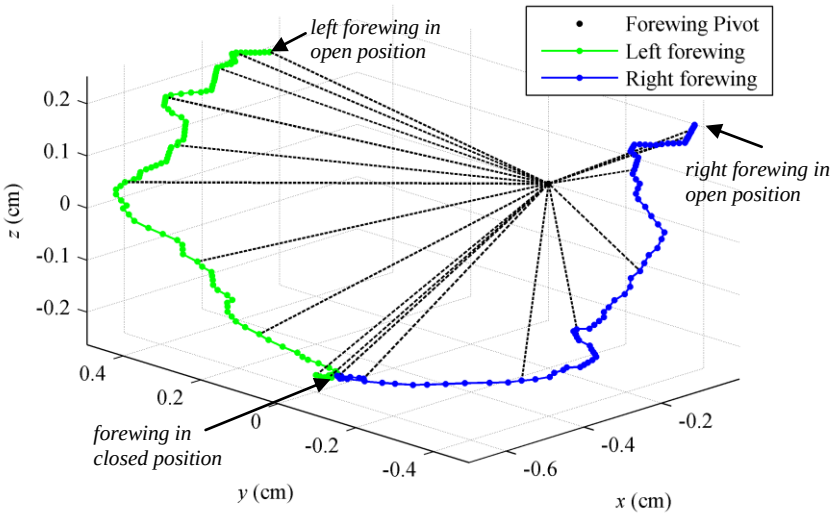

Figure 13. 3-D quantification of ladybug forewings.

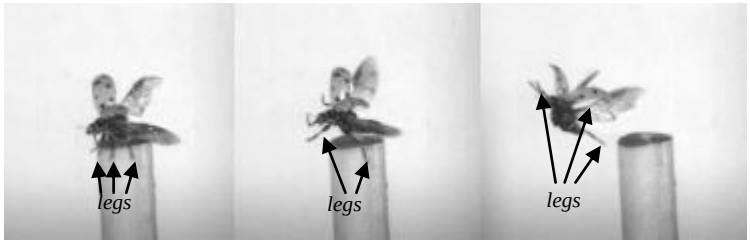

Figure 14. Image sequence showing ladybug leg extension.